ACADEMIA ROMÂNĂ
Revue Roumaine de Chimie
http://web.icf.ro/rrch/

Rev. Roum. Chim.,
2010, *55*(5), 319-328

STRUCTURE AND BEHAVIOUR OF CERAMIC MATERIALS BASED ON SnO_2 USED AS INERT ANODES IN ELECTROWINING PROCESSES

Ana Maria POPESCU,[a] George NIPAN,[b] Suzana MIHAIU,[a] Virgil CONSTANTIN,[a]
Mircea OLTEANU[a] and Nikolai SHUMILKIN [c]

[a] Roumanian Academy, "Ilie Murgulescu" Institute of Physical Chemistry, Splaiul Independentei 202, Bucharest., Roumania
[b]Russian Academy of Science," Kurnakov" Institute of General & Inorganic Chemistry, Leninsky pr.31, Moscow 119991, Russian Federation
[c] Russian Academy of Science,"A.A.Baikov" Institute of Metallurgy and Material Science, 8, Leninsky pr.49, Moscow 119361, Russian Federation

Received February 17, 2009

In this paper are presented studies on SnO_2 – based ceramics a new possible material for inert anodes. Results on structure and behavior of this material are discussed. By constructing the *x-y-z* diagram of ternary $SnO_2 – Sb_2O_3 – Cu_2O – O$ system, we could separate 5 monovariant equilibriums with SnO_2 -solid solution and vapour. From the compositions range of the ternary SnO_2-Sb2O3-CuO system we choose only 2 for the electrochemical studies. The measurements of decomposition potential (E_{dec}), current efficiency, cyclic voltammetry (CV) and corrosion were used to investigate these materials as inert anodes in a cryolite-alumina melt used for aluminum Hall-Heroult process at 970-1000°C. From the obtained data we conclude that the anodic process on these anodes takes place by a very simple process with no secondary reactions. Low alumina concentrations led to catastrophic corrosion of these anodes and the corrosion rate was found to increases with increasing current density. The corrosion rate of SnO_2-based anodes showed only a slight increase (of 0.0004 gcm^2h) when the anode-cathode distance was decreased from 5 to 2 cm. The mechanism of corrosion was elaborated by correlating the corrosion data with solubility data of SnO_2 – anodes in the Hall-Heroult bath.

INTRODUCTION

The only commercial process in use for making aluminium is the Hall-Heroult process, named after its inventors in 1889. Inert anodes have been considered for years to be the future of aluminum production by the Hall-Heroult process.

The designation of "inert anode" is being used to represent any oxygen-evolving anode. With such anodes the primary cell reaction, which in the Hall-Heroult process is:

$$1/2Al_2O_3 + 3/4\ C = Al + ¾\ CO_2 \qquad E_{rev} = 1.169V \qquad (1)$$

is changed to:

$$1/2Al_2O_3 = Al + 3/4O_2 \qquad E_{rev} = 2.196V \qquad (2)$$

The use of non-consumable anodes generates during electrolysis only oxygen, which environmentally is a very favourable gas and so the consumption of anode carbon in the electrolytic process will be eliminated. At the same time by using an non-consumable anode the emission of the green gases CO_2, CO, CF_4, C_2F_8 and most of the sulfurous gases (SO_2,COS, CS_2, H_2S) will be also eliminated and the process of producing aluminum will be an ecological one.

* Corresponding author: popescuamj@yahoo.com

The anode material is inert in the sense that it is not consumed in the cell reaction, as carbon anode is. However, as is demonstrated in the following, the materials in question undergo a slow corrosion, i.e. they are not completely inert; hence the designation "non-consumable" or "oxygen-evolving" may be more appropriate. The rate of deterioration is an important factor in their ability to compete economically with the well established carbon anodes.

The principal requirements for inert anodes are good electronic conductivity and chemical stability versus the electrolyte and the oxygen gas. For its resistance to chemical attack by pure oxygen (at 1 atmosphere pressure and 960°C) the choice of a fully oxidized material is appealing. Adding to this a high melting point and wide range of electrochemical stability and it is easy to see why ceramics have received attention. Almost exclusively, metallic oxides have been chosen as candidate materials for non-consumable anodes.

The purpose of this paper is to examine the structural and electrochemical factor governing the behavior of the SnO_2-ceramic based anodes. Tin oxide is the focus of attention owing to its high electronic conductivity. Taking in account the literature and personal data[1-9] we selected only the rich domain of SnO_2 having as best dopants Sb_2O_3 and CuO. It was already established[3] that CuO increases the densification and Sb_2O_3 increases the electrical conductivity (only in the presence of CuO) of the SnO_2 –based ceramic. Taking in account all our previous studies on SnO_2-based ceramics[3-9,20-21] two samples (S1 and S2) of SnO_2-based anodes having different composition were used in this study.

This paper examines the following aspects of SnO_2- ceramic based anodes: (1)Construct the x-y-z concentration diagram for the quaternary system SnO_2-Sb_2O_3-CuO-O and make correlation of structure and behavior of those ceramic materials; (2)Determine the structural and ceramic characterization of 2 samples (S1 and S2) chosen from the whole composition range of the studied system; (3)Study the electrochemical behavior of the two studied samples and to correlate it with the microstructure and solubility of SnO_2 in cryolite-alumina melt.

RESULTS AND DISCUSSION

Taking into account literature data[10-15] the concentration x-y-z diagram of quaternary SnO_2-Sb_2O_3-Cu_2O-O system was constructed applying the principle of continuity and conformity, supposing that every phase state of the system has the alone geometric image.

Studying the Figure 1, we can separate 5 monovariant equilibriums with SnO_2 – solid solution and vapour, which consists mainly from O_2, SnO and Sb_4O_6 molecules, for this system in the *P-T*- region 600 -1500 K and 10^{-2} – 10^5 Pa:

$$SnO_2(ss) – CuO – Cu_2O – CuSb_2O_6 – V \text{ (vapour)} \quad (3)$$
$$SnO_2(ss) – Cu_2O – Cu_4SbO_{4.5} – CuSb_2O_6 – V \quad (4)$$
$$SnO_2(ss) – Cu_4SbO_{4.5} – CuSb_2O_6 – Sb_2O_4 – V \quad (5)$$
$$SnO_2(ss) – Cu_2O – Cu_4SbO_{4.5} - Sb_2O_4 – V \quad (6)$$
$$SnO_2(ss) - Cu_2O – Sb_2O_3 – Sb_2O_4 – V \quad (7)$$

Really the compositions of SnO_2(ss) in the monovariant equilibrium (nonvariant points on surface, which borders SnO_2 –solid solution) differ from one to another. The most important contribution to the structural changes of those ceramics is due to the formation of $CuSb_2O_6$ compound, which during the thermal treatment we will prove that can form $Cu_4SbO_{4.5}$.

The obtained data from the structure study are in very good agreement with previous data[3,7,10,13-17] regarding the structure of SnO_2-based ceramic anodes. The most important contribution to the structural changes is due to the formation of $Cu_4SbO_{4.5}$, as we will present below.

The initial nominal composition of the chosen samples for this study (labeled S1 and S2) along with the phase composition and microstructure determined by XRD are presented in the Table 1.

After thermal treatment, X-ray diffraction data indicate the formation of the rutile type solid solution (SnO2(ss)) as unique phase (Table 1) , the Cu/Sb ratio of the samples is >1 and $Cu_4SbO_{4.5}$ formation may occur[13,18]. Must be notice that this compound does not dissolve into the SnO_2 lattice; the $CuSb_2O_6$ binary compound, at ~1100°C, is solved in SnO_2 up to 25 mol% as $Cu_{1/3}Sb_{2/3}O_2$. The solid solutions formed have a rutile-type structure.[10,13]

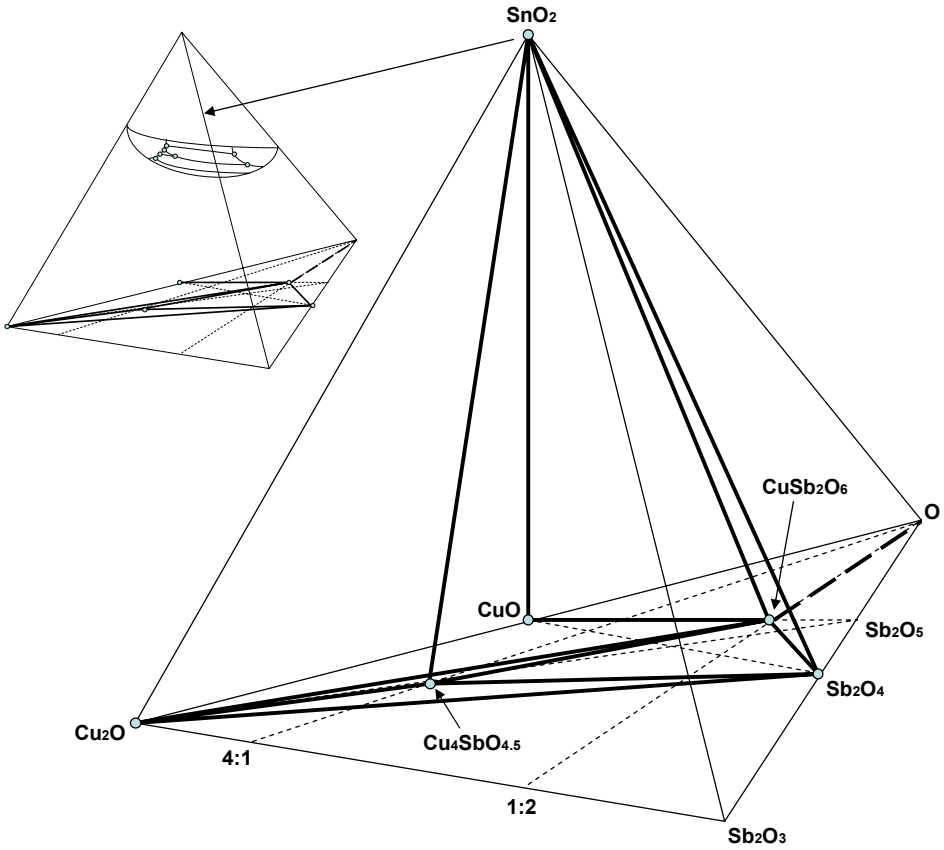

Fig. 1 – The *T-x-y-z* diagram of ternary SnO_2 – Sb_2O_3 – Cu_2O – O system.

Table 1

Initial composition, phase composition and microstructure of the studied samples

Sample	Composition wt%	CuO/Sb_2O_3 molar ratio	Phase composition	Microstructure
S1	$98SnO_2$-$1Sb_2O_3$-1CuO	3.7	$SnO_{2(ss)}$	$Cu_4SbO_{4.5}$
S2	$96SnO_2$-$2Sb_2O_3$-2CuO	3.7	$SnO_{2(ss)}$	$Cu_4SbO_{4.5}$

In fact during the thermal treatment the following reactions take place:

$$\sim 500^{\circ}C: \quad Sb_2O_3 + 1/2O_2 \rightarrow Sb_2O_4 \tag{8}$$

$$<900^{\circ}C: \quad Sb_2O_3 + CuO + 1/2O_2 \rightarrow CuSb_2O_6 \tag{9}$$

$$940^{\circ}C: \quad CuSb_2O_6 + 7CuO \rightarrow 2\,Cu_4SbO_{4.5} + 2O_2 \tag{10}$$

$$1100^{\circ}C: \quad [1-(x+y)]SnO_2 + xSb_2O_4 + yCuSb_2O_6 \rightarrow SnO_{2(ss)} \quad ; x + y \leq 1 \tag{11}$$

$$(1-x)SnO_2 + xCuSb_2O_6 \rightarrow SnO_{2(ss)} \quad ; x \leq 0.5 \tag{12}$$

$$xSnO_2 + (1-x)CuSb_2O_6 \rightarrow CuSb_2O_6(ss) \quad ; x \leq 0.2 \tag{13}$$

The SnO_2-based solid solutions become unstable over >1200°C (in air) and the following decompositions may occur: [13,19]

$$SnO_{2(ss)} \rightarrow SnO_2 + CuSb_2O_6 \tag{14}$$

$$2Cu_4SbO_{4.5} \rightarrow 4Cu_2O + 7/2Sb_2O_3 + 9/2O_2 \tag{15}$$

Solubilization reactions of Sb_2O_4 and $CuSb_2O_6$ in the $SnO_{2\ lattice}$ were evidenced by XRD measurements, which show only the existence of $SnO_{2(ss)\ even}$ if the quantities of Sb_2O_4 and $CuSb_2O_6$ (with different crystallization systems comparing with SnO_2) are over the limit of detection of the XRD equipment used.

During electrolysis (~950-980°C), because of the oxygen evolving at the anode, other reactions may take place:

$$2CuSb_2O_6 + 8CuO + 1/2O_2 \rightarrow Cu_9Sb_4O_{19} \quad (16)$$

$$Cu_9Sb_4O_{19} \rightarrow Cu_4SbO_{4.5} + 1/2CuSb_2O_6 + 3/2O_2 \quad (17)$$

The $Cu_9Sb_4O_{19}$ compound has a cubic structure with a_0=0.9620 nm lattice parameters.[19]

The surface of the sample is practically covered with a layer of the $Cu_4SbO_{4.5}$ compound. Under working conditions anyone of the above reactions can be promoted and these phase changes seem to be responsible for the electrochemical behavior of these anodes.[7,17,19-21]

The values of ceramic properties [shrinkage ($\Delta l/l$), porosity (P_a), and relative density (d_r)], electrical conductivity (K) at 1243K, activation energy for the electrical conductivity (ΔE_Λ) (determinate with an Arrhenius type relation) and Seebeck coefficients (C_S)] for studied samples S1 and S2 are given in Table 2. These data indicate good electronic conduction for both samples. It was also noticed that the electric resistivity of the studied samples decreases with increasing of temperature and current density. The small negative values of the Seebeck coefficients confirm the n-extrinsic semi-conductivity of these samples. The Arrhenius behavior of electrical conductivity in the 473-873K temperature range evidences the electronic type conduction.

Table 2

Ceramic, physical and electrical characteristics of the studied samples

Sample	Ceramic Properties			K_{1243K} (Ωcm^{-1})	$\Delta E_{473-873K}$ (eV)	C_s (μVk^{-1})
	$\Delta l/l$ (%)	P_a (%)	$d(gcm^{-3})$			
S1	-18.0	0	6.54	0.748	0.50	-1.83
S2	-11.3	0	6.55	0.823	0.25	-1.78

*$\Delta l/l$=Shrinkage ; Pa=Porosity ; d=Density; K=Conductivity; ΔE=Activation energy; Cs=Seebeck coefficient

Our main purpose was to see if these materials are suitable for using as inert anodes in the Hall-Heroult process for aluminum electrolysis. That is why the two samples were tested in the cryolite-alumina laboratory electrolysis bath (composition and conditions are presented in the Experimental part), from the point of view of their electrochemical behavior. In order to make a complete electrochemical study we started with the polarization curves, determined the decomposition potential which was subsequently correlated with cyclic voltammograms and finally we looked for the evolution of current efficiency and corrosion of the studied SnO_2-based anodes. A cyclic voltammetry study on the solubility of SnO_2 in the electrolysis bath was also carried out.

From the polarization curves, registered for S1 and S2 in comparison with Pt-anode, we can observe that both S1 and S2 show similar behaviors as inert Pt anode. For a current density of $0.5Acm^{-2}$ the S2-anode gives cell voltage of ~4V, values almost identicall with Pt-anode, which is in accordance with literature[22] and with what we expected, as S2 has the highest density and conductivity.

Starting from the observation that the S1 and S2 have so similar voltages and because S2 has values comparable with Pt-anode, we decided to use only the sample S2 for the other electrochemical measurements.

The decomposition potential (E_{dec}) was determined by using the classical I-U curves.[23] From the data presented in Figure 2A we calculated the E_{dec} as being equal to ~2.17V which corresponds rather closely to the standard *emf* = 2,20V for the reaction of alumina decomposition (eq.2). Also it is important to see that the data obtained for S1 and S2 are very close to those on Pt (2,18V).

From polarization data it was found that on these anodes as on Pt, the values of potential ohmic drop (E_Ω) are almost equal with the Faradays'ohmic drop. So we can assume that the "superficial state" of the SnO_2-based anodes is comparable with that of Pt from the point of view of umectability and electrochemical activity. In the same time this means that the connection we made between the SnO_2-based anode and the metallic conductor assures a good pure ohmic contact.

The measured overvoltage on S1 and S2 anodes was found to be almost the same, having a very low value of ~0.14V and being 4-6 times lower than that on carbon anodes. This behavior, correlated with the ceramic properties of the studied samples, confirms an interdependence of the overvoltage with the porosity of the studied materials.[24,25]

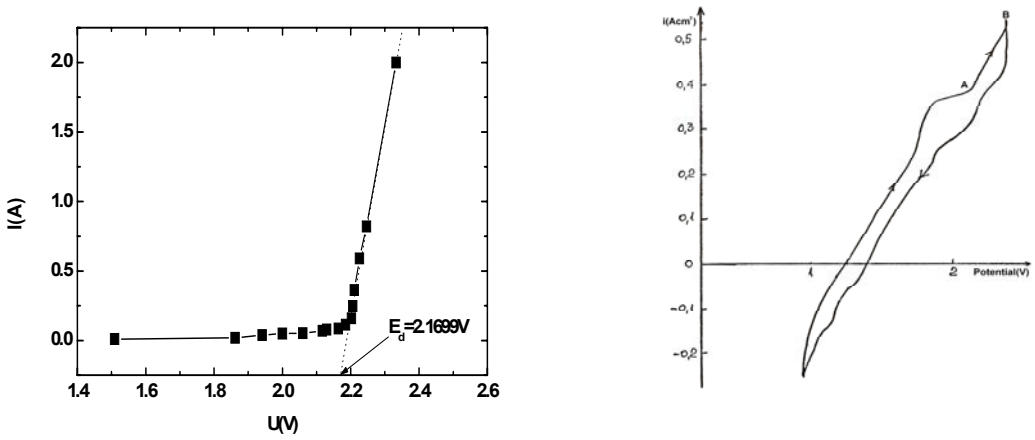

A **B**

Fig. 2 – Electrochemical data obtained on S2-anode in Na_3AlF_6-CaF_2-Al_2O_3 melt at 980^0C and $0.8Acm^{-2}$:
A. I-U curves for experimental determination of decomposition potential;
B. cyclic voltammogramm obtained with RE=Al/Al^{3+}, CE= graphite and
at $v=400mVs^{-1}$ (A-B = Al_2O_3 decomposition, B-C = oxygen evolution).

Cyclic voltammetry study has been performed in cryolite-alumina melt for S1 and S2 anodes (Figure 2B) and compared with the literature data for carbon anodes (graphite). Very fast cyclic voltammetry measurements ($>5Vs^{-1}$) conducted on graphite in cryolite-alumina melts showed the presence of an anodic peak prior to the peak associated with CO_2 formation.[26] In fact, 5 distinct peaks are present on the voltammogram, which were attributed to adsorbion/desorbtion of oxygen forming a carbon-oxygen surface compound. The shape of this voltammogram expresses the complexity of the anodic process on these carbon anodes.The evolution of voltammograms with SnO_2-based anodes (obtained using a reference electrode (RE) Al/Al^{3+}) showed once again a great difference in the electrochemical behavior of these anodes and carbon one. The voltammogram obtained with SnO_2-based anodes (Figure 2B) presents only one anodic peak at ~2,178 V, which corresponds to the value of the alumina electro-reduction potential (E_{rev}=2,19V).

Comparing the two anodic processes on carbon and SnO_2-based anodes, one can see the simplicity of the anodic process on SnO_2-based anodes.

Taking into account the criteria for voltammo-grams diagnosis criteria [27-33] and looking to the obtained data, we can conclude that the discharge of oxygen on the SnO_2-based anode is a reversible reaction controlled by diffusion as evidenced by the linearity between the peak current (i_p) and the square root of the scanning rate ($v^{1/2}$) as presented in Figure 3.

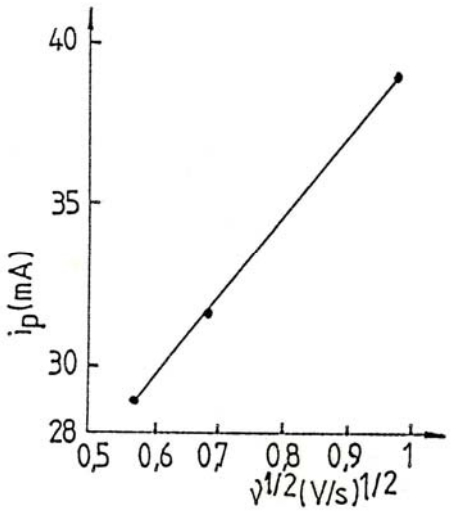

Fig. 3 – Dependence of the anodic peak current (i_{pa}) on square root of the scan rate ($v^{1/2}$)
for the cyclic voltammogrames recorded in a cryolite-alumina melt at 980^0C with S2-anode.

We calculated the number of electrons implicated in the anodic process starting from the relation:

$$n \quad 2.30\frac{RT}{E_p F} \qquad (18)$$

where: $\Delta E_p = E_{p(a)} - E_{p(c)}$,n= number of exchanged electrons. This relation is applicable for reversible reactions with separation of insoluble products on electrodes. Taking into account the following data obtained from the voltammogram in Fig.2B: T=970°C, v=0.4Vs^{-1}, $E_{p(a)}$ = 2.192 , $E_{p(c)}$ = 1.905 and ΔE_p=0.287, it results that by applying eq.18 the number of electrons implicated in the anodic process is n~2, which means that the discharge of oxygen on the SnO_2-based anode takes place with the exchange of 2 electrons and without any secondary reactions.

The voltammograms obtained with a quasi reference electrode (QRE) of Pt, showed a significant residual current at potentials below the oxygen evolution potential. Such a residual current was also found by Xiao[34] and it was presumed that was due to anodic oxidation of Sb^{3+} and Sb^{2+} ions, formed by the dissolution of the anode in the melt:

$$Sb^{3+} \rightarrow Sb^{4+} + e \qquad (19)$$

$$Sb^{2+} \rightarrow Sb^{4+} + 2e \qquad (20)$$

This residual current could also be due to the oxidation of the metal (Al or Na) dissolved in the melt.

Literature data[22,35] show that during the aluminum electrolysis with SnO_2-based inert anodes, the bath and aluminum metal were somehow contaminated with tin.

As one of the limiting factors of any industry is the energy requirement and as the electrochemical processes are big energy consumers, it is obvious that an important parameter for technology is the current efficiency. A significant problem for the application of inert anodes is the current efficiency with respect to aluminum. A complete study on the current efficiency for S2 anodes is presented in Figure 4.

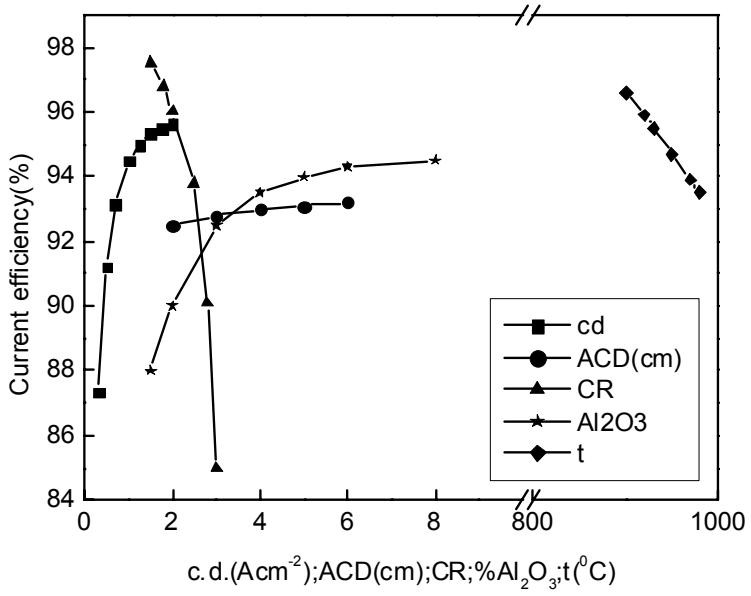

Fig. 4 – Evolution of the current efficiency of S2 with current density (cd), anode-cathode distance (ACD), cryolite ratio (CR=molNaF/molAlF$_3$), concentration of Al_2O_3 in the electrolyte bath and the temperature (t).

The obtained data for the current efficiency proved that SnO_2-based anodes gave higher current efficiency (>95%) that did the carbon anodes (86-92% and 96% in some new modern cells) and these data are in good agreement with literature.[22,36-38]

The current efficiency decreases with increasing temperature (t) in the electrolyte and increases monotonously with increasing the current density (cd) in the range 0.5-2A, but do not change significantly when reducing the anode-cathode distance (ACD) from 4.5 to 2.2cm. The oxygen bubbles formed on the inert anode are much smaller that CO_2 on carbon anodes and this permits the ACD to be reduced. The current efficiency is rising with the addition of Al_2O_3 and is lowering by the increasing of the cryolite ratio (CR=molar NaF/AlF$_3$). At low alumina concentration and at high current densities "catastrophic corrosion" phenomenon was observed. This takes place at the

decomposition potential of SnO_2, whereby SnO_2 provides oxygen for the anode reaction.[39]

The corrosion resistance may be the most important property in determining the performance of inert anodes. For this reason corrosion of inert anodes has been studied extensively.[22]

There are several processes that can lead to corrosion and possible destruction of inert anodes, but the most important is the dissolution of the component oxides in the electrolyte. Our results on the corrosion of sample S2 are presented in Figure 5.

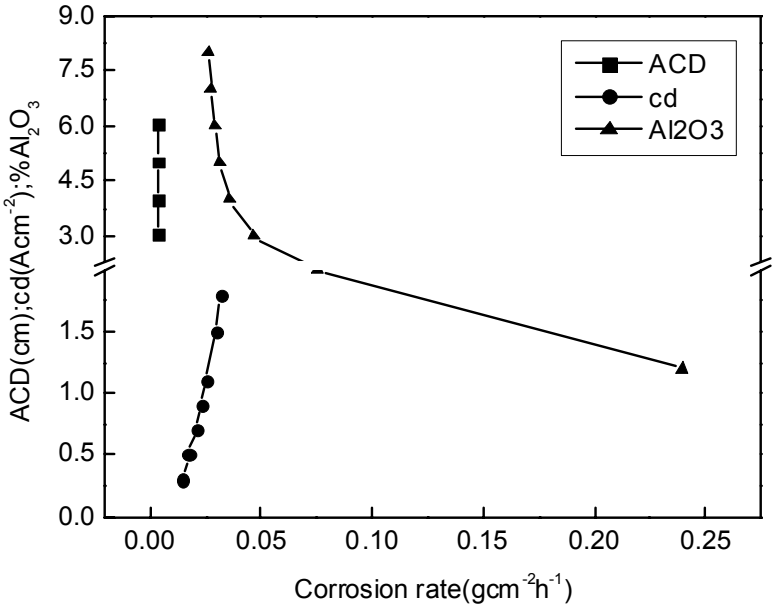

Fig. 5 – Corrosion rate of S2 as a function of the current density (cd), anode-cathode distance (ACD) and wt% Al_2O_3 .

It can be seen that the corrosion rate increases with increasing current density. As the current efficiency also has been demonstrated that increases monotonously in the same direction, it is recommended to work at current densities of 0.5-0.8Acm^{-2}. When the bath was saturated with alumina, no corrosion degradation was observed at high current densities. From the point of view of the anode-cathode distance, there is no significant influence by decreasing ACD until 2 cm. We also found that the corrosion rate increases slowly with decreasing Al_2O_3 concentration in the electrolysis bath. Below 1% (w/w) Al_2O_3 the so-called catastrophic corrosion occurred, while at concentrations above 6% (w/w) Al_2O_3 the corrosion reached acceptable levels. These results are in good agreement with the results found in literature.[22,36,39]

As by visual inspection no visible corrosion was observed on the S1 and S2 anodes after electrolysis, SEM investigations where done on sample S2 of anode after electrolysis (Figure 6). The active surface is seen on the left side of the picture. As no visible changes in porosity were found it seemed that the interior of the anode was not unaffected.

These results are in good agreement with literature[39], where the XRMA measurements did not detect any Al, Na or Ca beneath the active surface of those anodes. It is therefore reasonable to assume that no appreciable penetration of bath into the anode has occurred.

In order to understand exactly the process of solubilization of SnO_2 and elucidate the mechanism of corrosion, a cyclic voltammetry study was perfomed in cryolite-alumina melts containing SnO_2 and the results are presented in Figure 7. One must take into account that the Pt quasi-reference electrode causes a shift in the absolute magnitude of the potential.

The obtained voltammograms are in good agreement with literature[40,41] and show the presence of two oxidation states of tin in the melt and correspondingly two reduction states, while the large increase in the anodic current at potentials higher than 1,1V corresponds to the fluorine evolution.

$$(\text{Red 2})\quad Sn^{4+} + 2e \rightarrow Sn^{2+} \qquad (21)$$

$$(\text{Red 1})\quad Sn^{2+} + 2e \rightarrow Sn \qquad (22)$$

$$(\text{Ox1})\quad Sn - 2e \rightarrow Sn^{2+} \qquad (23)$$

$$(Ox2) \quad Sn^{2+} - 2e \rightarrow Sn^{4+} \qquad (24)$$

$$2F^{-} + 2e \rightarrow F_2\uparrow \qquad (25)$$

So by the dissolution of SnO_2 in cryolite-alumina melts tetravalent tin species are formed, being reduced to divalent tin under reducing conditions and further to metallic tin.

During electrolysis with SnO_2 –based anodes the condensate above the melt contained both divalent (SnF_2) and tetravalent (SnO_2) tin species.[41]

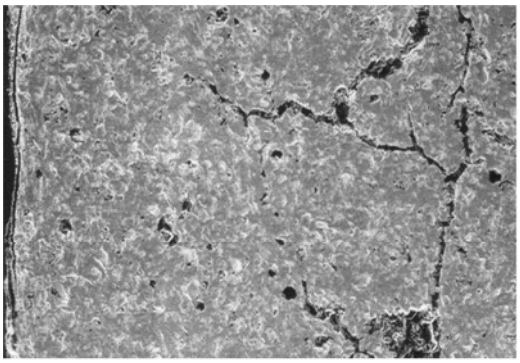

Fig. 6 – The SEM micrograph image of the active surface of S2 inert anode after electrolysis.

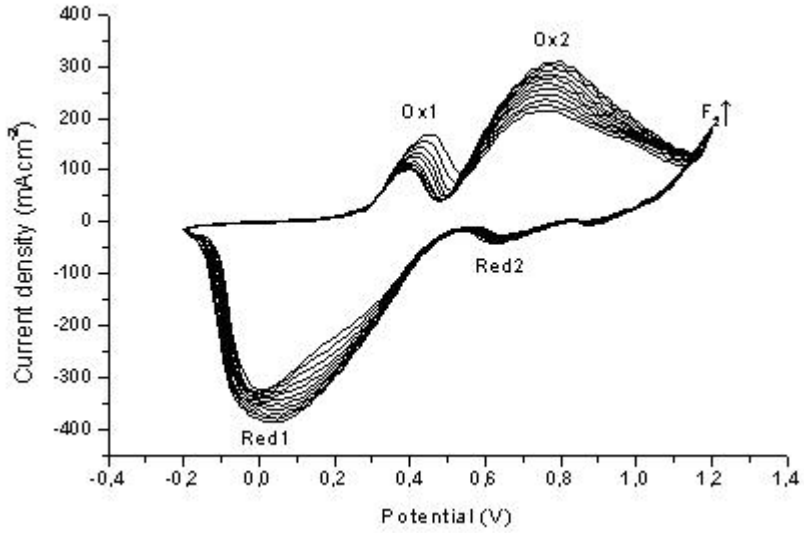

Fig. 7 – The cyclic voltammogram obtained for the solubility of S2 inert anode in cryolite-alumina melt at 980^0C; QRE=Pt wire (ϕ=2mm), CE=GC wire ((ϕ=2mm); v=50-200mVs^{-1}.

Taking into account all literature data[17,22,34,36] and our personal ones obtained on corrosion of SnO_2-based anodes, it is clear that one obvious mechanism of corrosion is the chemical dissolution of the anode material, according to the reaction:

$$SnO_{2\,(s)} + 4/3AlF_3 = SnF_{4\,(diss)} + 2/3\ Al_2O_3 \qquad (26)$$

$$SnF_{4(diss)} + 4/3Al = Sn + 4/3AlF_{3(diss)} \qquad (27)$$

Another possible corrosion mechanism is the reduction of tin oxide by the dissolved metal, according to the following reaction:

$$SnO_{2(s)} + 4/3Al_{\,(diss)} = Sn + 2/3Al_2O_3 \qquad (28)$$

Reducing of SnO_2 by the $Al_{(diss)}$ from the electrolyte can take place when the anodic current density is low and in this case $Al_{(diss)}$ can reach with the anode surface reducing the oxide material, which explains the increase in corrosion rate at anodic potentials below 2V, as indicated in Fig.5.

Correlating the corrosion study with the structure and microstructure of those anodes, we conclude that formation during the thermal treatment of the $Cu_4SbO_{4.5}$ compound is responsible for the destruction of these types of anodes.

However for industrial applications the corrosion rate of inert anodes should be maximum 1cm/year. This corrosion rate is acceptable from the point of view of anode lifetime, but for some impurities it may not be acceptable due to

contamination of the aluminium metal. It seems that tin is one of the elements that is unwanted in aluminium because it forms a separate, low-melting phase.

EXPERIMENTAL

For the obtaining of the ceramic based inert anodes S1 and S2 we used SnO_2, Sb_2O_3 and CuO from Merck and Fluka (p.a).The preparation method was presented in detail in previous papers.[3,6]

For the obtained pellets, the densification degree was evaluated from: linear shrinkage ($\Delta l/l$ - %), by measuring the variation of the sample diameter before and after the thermal treatment; apparent porosity (P %), by weighing thermally treated samples before and after 24 hrs immersion in toluene.

To investigate the internal morphology of the samples, the surfaces and fracture of the sintered ceramics were observed by Scanning Electron Microscopy (SEM JEOL 32 type).

A direct current bridge was used for electrical conductivity measurements (four points scheme) on the gold - coated pellet.[17]

The Seebeck coefficient was measured at room temperature (warm point method, platinum reference).

All experimental methods for determining the ceramic, physical and electrical properties of those SnO_2-based anodes (working electrodes= WE) were presented in details elsewhere.[3,7,16,19]

The electrochemical studies were performed in an electrolyte of composition: Na_3AlF_6 (CR=molNaF/AlF_3 =2.7) +5wt%Al_2O_3 +5wt%CaF_2 at 970-990°C.

The polarization measurements were performed under galvanostatic conditions at 980^{0}C. The anodic overvoltage was determined vs. Al/Al^{3+} reference electrode, by slow potential steps (3step/min, 20A/step), without correction of the ohmic drop.

The voltammetric studies were done using two types of potentiostats (Tacussel 10-20X with an X-Y Endine registrator and VoltaLab080-Radiometer with Volta Master 4 software). As reference electrode (RE) Al/Al^{3+} was used and Pt (quasi RE) and as auxiliary electrode (AE) pure graphite rod or the graphite crucible was used.

The measurements of the current efficiency were done by collecting the total amount of the evolved anodic oxygen gas, as presented in details in previous pappers.[27,28] The corrosion rate was determined by the gravimetric method.[6]

CONCLUSIONS

This study proved that the most important compound formed in the quaternary system SnO_2-Sb_2O_3-CuO-O is $CuSb_2O_6$ which during the thermal treatment is then transformed in $Cu_4SbO_{4.5}$. This appears on the surface of the anode and represents grains for solubility /corrosion during the aluminum electrolysis. The current efficiency and corrosion rate pointed out the conditions of high current efficiency and low cryolite ratio during Al electrolysis with those anodes. The electrolyte should have fairly high %Al_2O_3 to minimize the corrosion and the cell must operate at medium current densities (0.5-0.8Acm-2). The great advantage of those anodes seems to be the possibility of operating at short ACD (~2 cm). Even if it is reasonable to assume that no appreciable penetration of the bath into the anode occurs, the solubility measurements showed that the dissolution was proportional with the composition of the anode and even if S1 and S2 had a good resistance to the corrosion, a slight solubility which contaminates the aluminium product took place.

Taking into account the good properties (ceramic & electrochemical) of these ceramic materials used as inert anodes we intend to use them in Mg, Ca and Fe electrolyses, which take place at lower temperature and with electrolytes not so aggressive as cryolite.

Aknowledgement: We acknowledge the partial financial support of this research by the Roumanian Academy under Grant 53/2007-2008.

REFERENCES

1. K.Grjotheim, K.Krohn, C.Malinovsky, M.Matiasovsky and J.Thonstad, "Aluminium Electrolysis- Fundamentals of the Hall-Heroult Process", 2nd edition, Aluminium Verlag, Dusseldorf, Germany, 1982.
2. H.Alder (Swiss Aluminium Ltd.), *U.S.Pat.* 3.960.678 (1976).
3. S.Mihaiu, PhD Thesis, "Structure and physico-chemical properties of the Sn-Sb-Cu-O", ICF-Bucharest, Roumania, 1998.
4. S M. Zaharescu, S. Mihaiu, S. Zuca and K. Matiasovsky, *J. Mater. Sci.* , **1991**, *26*, 1666.
5. S. Zuca, M. Terzi, M. Zaharescu and K. Matiasovsky, *J. Mater. Sci.*, **1991**, *26,* 167.
6. A.M.Popescu ,S.Zuca, S.Mihaiu and V.Constantin, *Anal.Univ.Buc.Physics*, **2000**, p. 93-102.
7. A.M.Popescu, S.Mihaiu and S.Zuca, *Z.Naturforsch.*, **2002**, *57a*, 71.
8. R.P.Pawlek, *Aluminium,* **1995**, *71,* 202 & 340.
9. S.Mihaiu, S.Zuca, A.M.Popescu, Gh.Aldica and M.Zaharescu, *Key Eng.Mater.,* 2002, *206-213*, 1481.
10. M. Zaharescu, S. Mihaiu, D. Crisan and S. Zuca, "3-rd Euro Ceramics",P. Duran & F. F. Fernandez Eds., Faenza, Editura Iberica *2*, 1993, p.359.
11. M. Stan, S. Mihaiu, D. Crişan and M. Zaharescu, *Eur.& Solid Inorg.Chem.*, **1998**, *35*, 254.
12. S. Mihaiu, O. Scarlat, C Radovici and M. Zaharescu, *Proc.6-th ECERS*, Brighton, U.K., 1999, *2*, 68.
13. S. Mihaiu, O. Scarlat, C. Radovici and M. Zaharescu, *Proc. 13-th Conf. Glass & Ceramic*, Varna, Bulgaria, B. Sarmoneva, S. Bacharova, I. Gutzov, I. Dimitrov Eds., Sofia, 1999, *2*, 75.
14. O. Scarlat, S. Mihaiu, M. Zaharescu, *J Eur Ceram.Soc.*, **2002**, 22, 1839.

15. E. A. Varella, D. Gonevea, E. Longo, N. Dolet, M. Orillon and E. P. Bonnet, *Diffus. Defect Data*, *Pt. B*, **1992**, 25.
16. A.M.Popescu, S.Zuca and S.Mihaiu, *NATO-ASI-Molten Salts from Fundamentals to Applications*, Kas, Turkey, **2001,** ST-12
17. A.M.Popescu and S.Mihaiu, *Proc.Int.Conf.Eng.Tech.Sc-Intern.Symp.Adv.Materials(ICET-ISAM),* J.Song&R.Yiu Eds., New World Press, Beijing, China, **2000**, *2*, 1156.
18. S.Shimada and K.J.Mackenzie, *Termochimica Acta,* **1982**, *56*, 73.
19. S. Shimada and T. Ishii, *Reactivity of Solids*, **1989**, *7*, 183.
20. A.M.Popescu, M.Gaune-Escard, S.Zuca, S.Mihaiu, V.Constantin and V.Malyovanyi, "EUCHEM 2004-Molten Salts Conference Proceedings", Eds. J.Kazmierczak & G.Zabinska-Olszak, Wroclaw, Poland, ISSN / 0239-6661, 2004, 278.
21. A.M.Popescu, S.Mihaiu, M.Zaharescu and V.Constantin, *J.Optoelectr.Adv.Mater. (JOAM),* **2007,** *9,* 2227.
22. I.Galasiu, R.Galasiu and J.Thonstad, "Inert Anodes for Aluminium Electrolysis", 1st edition, Aluminium-Verlag, Dusseldorf, Germany, 2007.
23. V.Constantin and A.M.Popescu, *Rev.Chim. (Bucharest),* **2005**, *56*, 1246.
24. A.M. Popescu, S. Mihaiu and V. Constantin, *ROMPHYSCHEM-12*, Bucharest, Roumania, **2006**, p. 110.
25. S.Zuca, C.Herdlicka and M.Terzi, *Electrochim.Acta,* **1980**, *25*, 211.
26. S.Jarek and J.Thonsdtad, *J.Electrochem.Soc.,* **1987**, *134*, 856.
27. R.S.Nicholson, *Electroanal.Chem.,* **1965,** *10,* 376.
28. R.S.Nicholson, *Anal.Chem.,* **1964**, *36*, 706.
29. J.M.Saveant, *Electrochim.Acta.,* **1965,** *10*, 905.
30. J.M.Saveant, *Electrochim.Acta.,***1967**,*12*, 1545.
31. M.S.Ihnman, *Anal.Chem.,* **1969**, *41,*142.
32. M.S.Ihnman, *Anal.Chem.,* **1970**, *42,* 521.
33. T.J.Kemp, "Instrumental Methods in Electrochemistry", Southampton Electrochemistry Group, Univer. Southampton, Ellis Horwood series in Physical Chemistry, ISBN 0-13-472093-8.
34. H. Xiao, R. Hovland, S. Rolseth and J. Thonstad, *Metall. Mater. trans.B,* **1996**, *27B,* 185.
35. E.Olsen, "Nikelferrite and tin oxide as anode materials for aluminium electrolysis", Engineer PhD Thesis, University of Thondheim, Norway, 1995.
36. J.Thonstad, P.Fellner, G.M.Haarberg, J.Hives, H.Kvande and A.Sterten, "Aluminium Electrolysis-Fundamentals of the Hall-Heroult Porcess", 3rd edition., Aluminium-Verlag,Dusseldorf,Germany, 2001.
37. A.M.Popescu and V.Constantin, *Rev.Roum.Chim*.,**1998**, *43*,793.
38. A.M. Popescu, *Z.Naturforsch.,***2001**, *56*, 735
39. H.Wang and J.Thonstad, "Light Metals", P.G.Campbell Ed.,TMS, Warrendale,PA, 1989, p.283.
40. L.Isaeva, J.Yang, G.M.Haarberg, J.thonstad and N.Aalberg, *Electrochim. Acta.,* **1997**, *42*, 1011.
41. J.H.Yang and J.Thonstad, *J.Appl.Electrochem.,* **1997**, *27*, 422.